Pattern Translation and Rotation in Uncorrelated Source Distributions for Multiple Beam Antenna Design

Rodney G. Vaughan, *Senior Member, IEEE*

***Abstract*— In the uncorrelated scenario model, a continuous source distribution illuminates a receiver with waves bearing signals that are uncorrelated with respect to their angle of arrival. This model is used for multipath situations such as scintillating atmospheres, but also can be applied to optical beams for indoor communications, acoustic beamforming, and, of particular interest here, mobile communications. For diversity antennas operating in such a scenario, patterns that produce uncorrelated signals are required. An angular separation of directive beams in multipath scenarios acts to decorrelate the received signals. It is of interest to quantify the minimum angular spacing required of beams in order to provide a framework for the design and configuration of the antennas. The approach is to consider only the main lobe of the antenna pattern and to take it as a real function. This is reasonable as long as most of the energy is conveyed via the main beam. In practice, the sidelobe structure and nonuniformity in the phase of an actual pattern act to improve the situation in the sense that the decorrelation angles become smaller. The conditions for angular diversity result in a simple rule-of-thumb for the minimum beam separation requirement, which is essentially independent of the directivity. Finally, both scalar (acoustic case and circularly polarized case) and vector (linearly polarized case) elliptic beams rotated about their boresight axes are analyzed for the decorrelation rotation angle as a function of the ratio of the ellipticity. The resulting design curves offer a guideline to beam configuration for multipath scenarios.**

***Index Terms*—Multibeam antennas.**

I. Introduction

THE use of multiple antennas is an established diversity technique for improving communications channel quality in multipath environments [1], [2]. The basic idea is to receive the wanted signal from multiple antennas that have mutually uncorrelated channel degradations and combine the received signals such that the resultant signal is less degraded than any of the individual channels.

The requirement of the antennas is, therefore, to provide uncorrelated channels. Under certain conditions, this requirement is the same as providing uncorrelated antenna patterns [3] or beams, which is used below. By dealing with generic beams, rather than specific antenna implementations such as arrays, reflector, surface wave, etc., the formulation gives generic results in terms of the antenna patterns. However, antenna-specific patterns can also be used and some results for directive antennas are compared below.

The *scenario* is the relationship between the incoming waves, $E_{\rm inc}(\theta,\phi)$, and the configuration of the receiving antennas and it is usually expressed as a time-averaged probability density function (pdf) referenced to the antenna coordinates. The scenario is normally considered uncorrelated in the sense that for each polarization

$$\langle E_{\rm inc}(\theta_1,\phi_1)E^*_{\rm inc}(\theta_2,\phi_2)\rangle = S(\theta,\phi)\delta(\theta_1-\theta_2)\delta(\phi_1-\phi_2) \tag{1}$$

where $S(\theta,\phi)$ is the time-averaged power density (per steradic square) distribution (i.e., the pdf) of incident waves. We also usually take the orthogonal polarizations to be uncorrelated. The modeled pdf and its uncorrelated nature are postulates which trade off simplicity, foster analytic progress, and reasonably represent the averaged physical situation. The two-dimensional (2-D) Clarke [4] scenario corresponds to a ring of dense sources (normally vertically polarized) on a horizon about the receiving antenna and it can be expressed as a power density of $1/(2\pi)$ per steradian from

$$S_C(\theta,\phi) = S_C(\theta) = \frac{1}{2\pi}\delta(\theta-\pi/2). \tag{2}$$

This scalar case can be duplicated and scaled for both polarizations. In this paper, we also use a Gaussian function to model a *directional scenario*.

In order to get "uncorrelated" channels from antenna ports, the correlation coefficient of narrowband fading signal envelopes should be lower than about 0.7, which corresponds to about a 1-dB loss (relative to that from a zero correlation) in the ideal two-branch diversity gain [5]. The envelope correlation coefficient ρ_e is approximately equal to the magnitude square of the complex correlation coefficient [5] of the open circuit signals denoted $|\rho|^2$, which is given in terms of the patterns by [3]

$$\begin{aligned}\rho_{12} &= \langle V_{O1}V^*_{O2}\rangle / \sqrt{\langle|V_{O1}|^2\rangle\langle|V_{O2}|^2\rangle} \\ &= \int_0^{2\pi}\int_0^{\pi} S(\theta,\phi)g_1(\theta,\phi)\cdot g_2^*(\theta,\phi)\sin\theta\, d\theta\, d\phi\end{aligned} \tag{3}$$

if g_1, g_2 are the normalized receiving patterns. For a single polarization, or the acoustic case, the dot product reduces to the scalar product.

Manuscript received September 30, 1996; revised March 25, 1998.

The author is with the New Zealand Institute for Industrial Research Limited, Lower Hutt, New Zealand.

Publisher Item Identifier S 0018-926X(98)05774-3.

The pattern diversity can be realized by the use of uncorrelated polarizations [6], [7], spatial separation of similar patterns [2], or angular separation of similar patterns [1]. With (3), all three degrees of freedom—polarization, spacing, and rotation—can be used together to realize uncorrelated patterns [8]. A design guideline can be developed for using a single degree of freedom. For example, using space diversity in the Clarke scenario, the open circuit voltage correlation coefficient function $J_0(k_0 d)$ goes to zero for omnidirectional patterns spaced by $d = 0.38$ wavelengths. A rule of thumb for space diversity in mobile communications follows as a half-wavelength separation between omnidirectional antennas [2] although much closer spacing is possible [9]. A guideline for angle diversity from antenna beams is the subject of this paper. The rule of thumb is found to be an angular spacing of half of the half-power beamwidth for a uniform scenario, although closer spacing is possible when sidelobe structure and phase nonuniformity are included.

The beams are modeled using Gaussian and cosine functions. Gaussian beams allow simple results but their approximation to a circular function causes the formulation to be best suited to medium and high directivities (see Section II). The cosine beams are more suitable for low directivities to be quantified. Two related approaches are taken for developing the angular spacing requirement for diversity from directive beams: the beam is considered in spherical polar coordinates with an angular pdf for the power density of the scenario; and the footprint of the beam on a plane (approximating the concave spherical surface) of uncorrelated sources is also considered. In Section III, the one-dimensional (1-D) case is first considered, followed by treatment of the 2-D, elliptic-shaped beams. In Section IV, the decorrelation by rotation of the elliptic beam is quantified. The following discussion section is a of the finite support of the circular coordinate system.

II. Correlation Operations in a Circular Support

In a correlation operation, the integration is bounded to $\phi \in [-\pi, \pi)$ for a circular beam pattern (function), $g(\theta, \phi)$, in circular coordinates. However, a noncircular function being correlated cannot be truncated at $\pm\pi$, even though the support of the pdf $p_\phi(\phi)$ is bounded at these limits. While integrals such as the centralized mean of a function $g(\phi)$ can be written

$$\mu_g = \int_{-\infty}^{\infty} p_\phi(\phi) g(\phi)\, d\phi = \int_{-\pi}^{\pi} p_\phi(\phi) g(\phi)\, d\phi \tag{4}$$

correlation-type integrals containing the form (here for the Clarke scenario $p_\phi(\phi) = 1/(2\pi)$)

$$\int_{-\pi}^{\pi} p_\phi(\phi) g(\phi + \Omega)\, d\phi = \frac{1}{2\pi} \int_{-\pi+\Omega}^{\pi+\Omega} g(\zeta)\, d\zeta \tag{5}$$

need to have $g(\phi)$ defined out to $\phi = \pi + \Omega$ and the operation becomes inconsistent with the support of the pdf. There are two ways to view the requirements of the beam function $g(\phi)$. Either $g(\phi)$ must repeat with period 2π as $|\phi|$ increases (circular functions), in which case there is no problem with the circular support; or a mapping of ϕ to $\tilde{\phi} \in [-\pi, \pi)$ must be employed to allow the use of more general (i.e., nonperiodic) functions which are then altered to be periodic via the form $g(\tilde{\phi}(\phi))$. Equivalently, it is useful for visualization to define a periodic function $\tilde{g}(\phi)$ from $g(\phi)$

$$\tilde{g}(\phi) = g(\tilde{\phi}(\phi)) = \sum_n g_n(\phi), \quad n = 0, \pm 1, \pm 2, \cdots \tag{6}$$

where

$$\begin{aligned} g_n(\phi) &= g(\phi + n2\pi) \quad (2n-1)\pi \le \phi < (2n+1)\pi; \\ &= 0 \qquad\qquad\quad \text{elsewhere} \end{aligned} \tag{7}$$

which gives the truncation of the nonperiodic function to form a periodic function. For circular functions, $g(\phi) = \tilde{g}(\phi) = g(\tilde{\phi})$.

Using $\tilde{g}(\phi)$ in the linear correlation, i.e., that with integral limits of $\pm\infty$, is the same as using it with the limits of the circular coordinate system support $[-\pi, \pi)$. So the angular correlation function for noncircular $g(\phi)$ in the circular support is

$$R_{\tilde{g}1\tilde{g}2}(\Omega) = \int_{-\infty}^{\infty} S(\phi) \tilde{g}\left(\phi + \frac{\Omega}{2}\right) \tilde{g}^*\left(\phi - \frac{\Omega}{2}\right) d\phi \tag{8a}$$

$$= \int_{-\pi}^{\pi} S(\phi) \tilde{g}\left(\phi + \frac{\Omega}{2}\right) \tilde{g}^*\left(\phi - \frac{\Omega}{2}\right) d\phi. \tag{8b}$$

More often than not, problems with reducing the integral occur because the mapping required for $(\phi - \Omega)$ does not allow separation of these two variables. In practice, it is convenient, therefore, to use circular functions for the pattern modeling in circular coordinate systems or else ensure that the mapping to a periodic function is unnecessary by maintaining

$$\frac{\gamma_B}{2} + \frac{\Omega}{2} < \pi \tag{9}$$

where γ_B is the effective support of the beam.[1] This condition keeps the beam effective support within the circular coordinate system support $[\pi, \pi)$ even when the beam is off center by half the correlation lag $\Omega/2$. More discussion about the condition is given for Gaussian beams in Section III. If the (9) is satisfied, then

$$R_{g1g2}(\Omega) = \int_{-\infty}^{\infty} S(\phi) g\left(\phi + \frac{\Omega}{2}\right) g^*\left(\phi - \frac{\Omega}{2}\right) d\phi \tag{10a}$$

$$\simeq \int_{-\pi}^{\pi} S(\phi) g\left(\phi + \frac{\Omega}{2}\right) g^*\left(\phi - \frac{\Omega}{2}\right) d\phi \tag{10b}$$

where the approximation sign $\simeq$ refers specifically to the approximation of neglecting the energy of the beam, which is outside of the effective beam support γ_B.

The preference for using these where possible in circular supports is obvious. In the case of the source distribution being on an infinite planar surface (see Section III-B), it is preferable to avoid modeling with circular functions on the plane since their periodic property creates periodicity in the

[1] The energy outside of γ_B is small enough to neglect in the correlation integral calculation.

planar correlation operation. (This is the opposite problem to using noncircular functions in a circular support.)

III. Angularly Spaced Beams in Circular Coordinates

A. 1-D Gaussian Beam with Gaussian Angular PDF

The source scenario is uncorrelated and also Gaussian within the support of a circular coordinate system. For a 1-D (single pattern cut) case, the scenario is denoted in the azimuth coordinate

$$S_G(\phi) = p_\phi(\phi) = K_s e^{-\frac{\phi^2}{2\sigma_s^2}}, \quad -\pi \le \phi \le \pi \tag{11}$$

where the mean angle (here meaning the direction of maximum power density) is taken as zero. The normalizing factor required to make $S_G(\phi)$ the pdf of the incident power is

$$K_s^{-1} = \sqrt{2\pi}\sigma_s \operatorname{erf}\left(\frac{\pi}{\sqrt{2}\sigma_s}\right). \tag{12}$$

The antenna amplitude pattern is denoted

$$\tilde{g}(\phi) = g(\phi) = e^{-\frac{\phi^2}{2\sigma_g^2}}, \quad -\pi \le \phi \le \pi. \tag{13}$$

The relation between the half-power beamwidth (HPBW) of a pattern and the Gaussian standard deviation parameter σ_g is

$$\text{HPBW} = \sigma_g 2\sqrt{2\ln\sqrt{2}}, \quad \text{i.e., } \sigma_g \approx 0.6 \text{ HPBW}. \tag{14}$$

To relate the beamwidth to the directivity, a 2-D beam must be considered. A circularly symmetric Gaussian beam is denoted using the zenith coordinate θ and has directivity

$$D_{\tilde{g}}(\sigma_g) = \frac{2}{\int_0^\pi e^{-\frac{\theta^2}{\sigma_g^2}} \sin\theta \, d\theta}. \tag{15}$$

The pencil beam directivity formula $D_p = 41\,000/(\text{HPBW})^2$ [10] is a good estimate, being within 0.5 dB as long as σ_g is less than 1 rad at which the directivity is $D_g = 6.75$ dB and $D_p = 6.51$ dB. Kraus' [10] formula for Gaussian beams (which is $0.88 D_p$) has improved accuracy for higher ($>\sim$ 8 dB) directivities only. The off axis directivity relative to its maximum value is

$$\left(\frac{g(\theta)}{g(0)}\right)^2 = \exp\left\{-\frac{1}{2(2\ln\sqrt{2})^2}\left(\frac{\theta}{\text{HPBW}}\right)^2\right\} \tag{16}$$

which gives, for example, a level of about -0.8 dB at an angle from boresight of quarter the HPBW.

The correlation function of the open circuit voltages resulting from the 1-D beams is

$$\langle V_{O1} V_{O2}^* \rangle = R_{g1g2}(\Omega) \simeq K_s K_c e^{-\frac{\Omega^2}{4\sigma_g^2}} \tag{17}$$

where

$$K_c = \sqrt{2\pi}\sigma_c \operatorname{erf}\left(\frac{\pi}{\sqrt{2}\sigma_c}\right) \tag{18}$$

and

$$\sigma_c^2 = \frac{\sigma_s^2 \sigma_g^2}{2\sigma_s^2 + \sigma_g^2}. \tag{19}$$

The Gaussian form of the correlation coefficient function is a result of the beams being Gaussian and the scaling constants K_c and K_S are a result of the (truncated) Gaussian scenario.

The extent of the beam is bounded by the sum of the beam effective support and the correlation lag being within the coordinate system support, i.e., $\gamma_B + \Omega < 2\pi$, from above. A conservative simple rule-of-thumb for the limit of the spread of the beam σ_g is obtained by maintaining the support γ_B as about $5\sigma_g$ radians (from $\pm 2.5\sigma_g$ radians about the centre of the beam), corresponding to 92% (from $\operatorname{erf}(2.5/2)$) of the energy of a centralized Gaussian beam being within the support and allowing the maximum correlation lag to equal twice the HPBW ($\approx 2 * 0.6\sigma_g$ radians). The bound follows as $5\sigma_g + 1.2\sigma_g < 2\pi$, giving a maximum standard deviation parameter for the beam function of $\sigma_g \approx 1$ rad or a maximum HPBW of about 95°. Note that this rule-of-thumb addresses the accuracy of an approximation within the mathematical formulation and does not account for inaccuracies of the Gaussian beam modeling a real-world beam. For comparison, a |sinc|-shaped beam has about 90% of its total energy (in the sense of having support of $\pm\infty$) within the support of its main lobe. For the beam function being well within the support, i.e., $\sigma_g \le\sim 1$ rad, corresponding to moderate and high directivities, there results $\sigma_c^2 \approx \sigma_g^2/2$ and $K_c \approx \sqrt{\pi}\sigma_g$.

The above rule-of-thumb is for a uniform scenario; for directive scenarios, the beams can be less directive. Using beams with lower directivity ($\sigma_g <\sim 1$ rad) results in the angular correlation coefficient function values increasing, especially for its smaller values. The decorrelation angle increases as a result. Lower directivities are better dealt with using cosine beams (see subsection *C.* below).

To find the correlation coefficient between the zero-mean signals from each beam we use

$$\rho(\Omega) = \frac{\langle V_{O1} V_{O2}^* \rangle}{\sqrt{\langle |V_{O1}|^2 \rangle \langle |V_{O2}|^2 \rangle}} = \frac{R_{g1g2}(\Omega)}{\sqrt{R_{g1g1}(\Omega) R_{g2g2}(\Omega)}}. \tag{20}$$

From the symmetry of the configuration, $R_{g1g1}(\Omega) = R_{g2g2}(\Omega)$, so the normalizing factor is

$$R_{g1g1}(\Omega) \simeq K_s K_k e^{-\frac{\Omega^2}{4(\sigma_g^2 + 2\sigma_s^2)}} \tag{21}$$

where

$$K_k = \sqrt{2\pi}\frac{\sigma_c}{2}\left(\operatorname{erf}\left(\frac{\pi - k\Omega}{\sqrt{2}\sigma_c}\right) - \operatorname{erf}\left(\frac{-\pi - k\Omega}{\sqrt{2}\sigma_c}\right)\right) \tag{22}$$

and

$$k = \frac{\sigma_s^2}{\sigma_g^2 + 2\sigma_s^2} = \frac{\sigma_c^2}{\sigma_g^2}. \tag{23}$$

The correlation coefficient function between the voltages is now established as

$$\rho(\Omega) \simeq \frac{\operatorname{erf}\left(\frac{\pi}{\sqrt{2}\sigma_c}\right)}{\frac{1}{2}\left(\operatorname{erf}\left(\frac{\pi - k\Omega}{\sqrt{2}\sigma_c}\right) - \operatorname{erf}\left(\frac{-\pi - k\Omega}{\sqrt{2}\sigma_c}\right)\right)} e^{-\frac{\Omega^2}{4}\left(\frac{1}{\sigma_g^2} - \frac{1}{\sigma_g^2 + 2\sigma_s^2}\right)}. \tag{24}$$

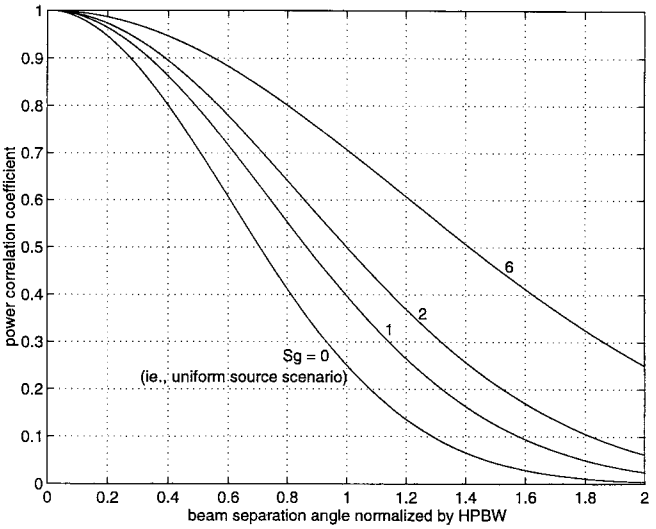

Fig. 1. The angular correlation coefficient function of the signal powers (similar to that of signal envelopes) for 1-D Gaussian beams spaced symmetrically with respect to the Gaussian scenario of uncorrelated sources. The abscissa is $S_g = (\sigma_g/\sigma_S)^2$ where σ_g is the spread of the amplitude beam and σ_S is the spread of the scenario (incident power).

If the two beams $g(\phi \pm \Omega/2)$ are well within the support of the scenario $S_G(\phi)$ [cf. the condition of (9)], then the correlation coefficient function is approximately Gaussian

$$\rho(\Omega) \approx e^{-\frac{\Omega^2}{2\sigma_\rho^2}} \tag{25}$$

where

$$\sigma_\rho^2 = \sigma_g^2\left(\frac{\sigma_g^2}{\sigma_s^2} + 2\right). \tag{26}$$

This equation relates the spread of the correlation coefficient function to that of the beam and the scenario. The power correlation coefficient, which is similar to the envelope correlation coefficient, viz., $|\rho(\Omega)|^2 \sim \rho_e(\Omega)$, is shown in Fig. 1 with the scenario spread σ_s as a parameter. As noted above, the HPBW has little influence as long as it is less than about 90°.

The limiting and special cases for the scenario are of interest. For a single incident wave $\sigma_s = 0$, which gives $\sigma_\rho = \infty$ and the correlation coefficient function is always unity independent of the beam (as long as it has nonzero gain). This can also be seen directly from the defining equation (10) with $S(\phi) = \delta(\phi)$. The result comes from the fact that for a single incident wave, the open circuit voltages of the two beams are simply scaled versions of the same signal. For the case of the scenario having the same spread as the beams $\sigma_s = \sigma_g$, then $\sigma_\rho = \sqrt{3}\sigma_g$, i.e., the correlation coefficient function has a spread of $1/\sqrt{3}$ of the spread of the beams. Similarly, for the spread of the scenario being the same as the spread of the power pattern $\sigma_s = \sigma_g/\sqrt{2}$, then $\sigma_\rho = 2\sigma_g$. For a uniform scenario, $\sigma_s \to \infty$ giving $\sigma_S \mathrm{erf}(\frac{\pi}{\sqrt{2}\sigma_s}) \to \sqrt{2\pi}$ and $S(\phi) = S_C = 1/2\pi$. This results in $\sigma_\rho = \sqrt{2}\sigma_g$, i.e., the correlation coefficient function has a spread, which is $\sqrt{2}$ times the spread of the amplitude beam.

The 0.7 decorrelation angle Ω_d can be defined as the angle for which $\rho_e = 0.7 \approx 1/\sqrt{2}$. For sufficiently directive beams this is found from

$$\rho_e(\Omega_d) \approx e^{-\frac{\Omega_d^2}{\sigma_\rho^2}} \tag{27}$$

$$\Rightarrow \Omega_d \approx \sigma_g\sqrt{\ln\sqrt{2}((\sigma_g/\sigma_S)^2 + 2)} = \mathrm{HPBW}\sqrt{\frac{1}{8}(\sigma_g/\sigma_S)^2 + \frac{1}{4}}. \tag{28}$$

When $\sigma_g/\sigma_S >\sim 3$ and, in particular, for the uniform scenario

$$\Omega_d = \frac{\mathrm{HPBW}}{2} \quad \text{(uniform scenario)} \tag{29}$$

i.e., the 0.7 decorrelation angle is half of the half-power beamwidth of the antenna pattern.

This simple result is independent of the pattern beamwidth as long as the beam is well within the circular support. In practice, the sidelobe structure and nonuniform phase of a real-world pattern will make the decorrelation angle smaller, so the above rule-of-thumb is interpreted as an upper limit for the minimum decorrelation angle for a uniform scenario. Fig. 1 (above) offers a feel for the effect of the spread of the scenario. For example, in the case where the power pattern has the same spread as the scenario, i.e., $(\sigma_S/\sigma_g)^2 = 2$, the 0.7 decorrelation beam separation increases from 0.5 to $1/\sqrt{2} = 0.7$ of the HPBW.

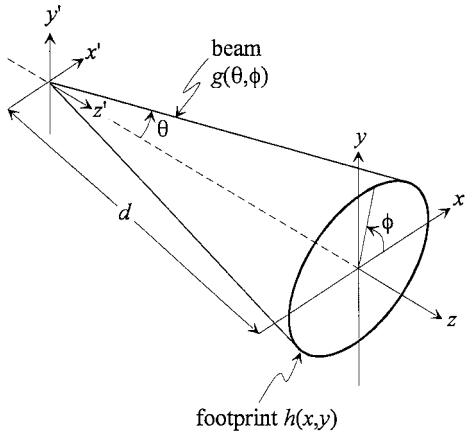

Fig. 2. The footprint in Cartesian coordinates from a beam.

B. Gaussian Footprint on a Plane

For an antenna being illuminated by a plane of uniform sources, a similar correlation expression can be derived for the translation of the beam. Traditionally, the term "footprint" is applied to satellite antennas illuminating the (convex spherical) earth, but the context is borrowed to recouch and extend to two dimensions the results of the previous section. Fig. 2 is a sketch of the beam coordinates. The beam is viewed here as receiving rather than transmitting, and reciprocity is assumed.

The relationship between the amplitude pattern of the beam $g(\theta, \phi)$ and the amplitude footprint on the plane xy, $h(x, y)$ is also depicted in the figure. If the beam is sufficiently narrow, then, for a small beam translation given by a change of Θ_0

in the zenith angle and a beam rotation given by a change of Φ_0 in the azimuth angle, the correspondence (denoted $\leftrightarrow$) between the footprint and the beam is

$$g(\Theta+\Theta_0,\Phi+\Phi_0)\leftrightarrow h(x+x_0,y+y_0) = h(x+d\sin\Theta\cos\Phi, y+d\sin\Theta\sin\Phi). \quad (30)$$

The small angle approximation allows the correspondence in translation distance on the plane to be proportional to the zenith angle change, i.e., $r_0=\sqrt{x_0^2+y_0^2}\propto\Theta_0$. The beam rotation is omitted here and addressed below in Section IV.

The footprint model is

$$h(x,y)=e^{-\left(\frac{x^2}{2\sigma_x^2}+\frac{y^2}{2\sigma_y^2}\right)} \quad (31)$$

where σ_x is the spread of the amplitude beam in the x direction and similarly for σ_y. Truncating the footprint to a support of $(\pm 2X,\pm 2Y)$, the correlation coefficient function for the voltages of two spaced beams is, cf. (25)

$$\rho(x_0,y_0)=K_{x,y}e^{-\left(\frac{x^2}{4\sigma_x^2}+\frac{y^2}{4\sigma_y^2}\right)} \quad (32)$$

where K_{xy} is given by (33), shown at the bottom of the page. When X,Y become large relative to σ_x,σ_y (footprint well within the scenario support), then $K_\rho\approx 1$. The significant aspect is that the x and y functions are independent

$$h(x,y)=h(x)h(y) \quad (34)$$

because of the postulate that the scenario is uncorrelated. So the 1-D decorrelation result of the previous section holds independently of the beam spread in the second dimension, (i.e., $\rho(x_0,y_0)=\rho_x(x_0)\cdot\rho_y(y_0)$) because of the assumption of the uncorrelated scenario and remains approximately Gaussian owing to the narrow beam assumption.

C. 2-D Cosine Beam

The cosine beam is an alternative model for the main lobe of a directive pattern. The 1-D amplitude pattern is written

$$g(\phi)=\cos^n\left(\frac{\phi}{2}\right) \quad (35)$$

which goes to zero at $|\phi|=\pi$ and is unity at $\phi=0$. The relationship between the HPBW and n is

$$\text{HPBW}=4\cos^{-1}\left(2^{-\frac{1}{2n}}\right)$$

i.e.,

$$n=-\log(\sqrt{2})/\log\cos\left(\frac{\text{HPBW}}{4}\right). \quad (36)$$

For very directive beams, the large n can lead to computational problems and it is better to scale the angle in order to reduce n and set the integration limits appropriately. The beam becomes $g(\phi)=\cos^n(m\phi)$ and the HPBW formulas modify accordingly.

The 2-D beam is written

$$g(\theta,\phi)=\sin^{n_\theta}\theta\cos^{n_\phi}\left(\frac{\phi}{2}\right) \quad (37)$$

which is directed along the x axis. For a uniform three-dimensional scenario, $S(\theta,\phi)=S_U=1/(4\pi)$ and the angular correlation function is

$$R_{g1g2}(\Psi)=\frac{1}{4\pi}\int_0^\pi \sin^{2n_\theta+1}\theta\,d\theta\int_{-\pi}^{\pi}\cos^{n_\phi}\left(\frac{\phi}{2}\right)\times\cos^{n_\phi}\left(\frac{\phi+\Psi}{2}\right)d\phi \quad (38a)$$

$$=\frac{1}{4\pi}I_s(2n_\phi+1)I_{cc}\left(n_\phi,\frac{\Psi}{2}\right) \quad (38b)$$

where

$$I_s(n)=\int_0^\pi\sin^n\theta\,d\theta=2\frac{n!!}{(n+1)!!},\quad n\in I,\ n\text{ odd}; \quad (39a)$$

$$=\pi\frac{(n-1)!!}{n!!},\quad n\in I,\ n\text{ even} \quad (39b)$$

and

$$I_{cc}(n,\gamma)=\int_{-\pi}^{\pi}\cos^n\left(\frac{\phi}{2}\right)\cos^n\left(\frac{\phi}{2}+\gamma\right)d\phi \quad (40a)$$

$$=\frac{\pi}{2^{2(n-1)}}F_n(n,\gamma) \quad (40b)$$

where

$$F_n(n,\gamma)=\sum_{k=0}^{\frac{n-1}{2}}\binom{n}{k}^2\cos(n-2k)\gamma,\quad n\in I,\ n\text{ even}; \quad (41a)$$

$$=\sum_{k=0}^{\frac{n}{2}}\binom{n}{k}^2\cos(n-2k)\gamma\cdot\varepsilon(n-2k),\quad n\in I,\ n\text{ odd} \quad (41b)$$

with

$$\varepsilon(m)=\frac{1}{2}\quad m=0; \quad (42a)$$

$$=1\quad m\neq 0. \quad (42b)$$

From the symmetry of the system, the normalizing factor is

$$R_{g1g1}(0)=\frac{1}{4\pi}I_s(2n_\theta+1)I_{cc}(2n_\phi,0) \quad (43)$$

$$K_{xy}=\frac{\left(\text{erf}\left(\frac{X+x_0/2}{\sigma_x}\right)-\text{erf}\left(\frac{-X+x_0/2}{\sigma_x}\right)\right)\left(\text{erf}\left(\frac{Y+y_0/2}{\sigma_y}\right)-\text{erf}\left(\frac{-Y+y_0/2}{\sigma_y}\right)\right)}{4\text{erf}\left(\frac{X}{\sigma_x}\right)\text{erf}\left(\frac{Y}{\sigma_y}\right)} \quad (33)$$

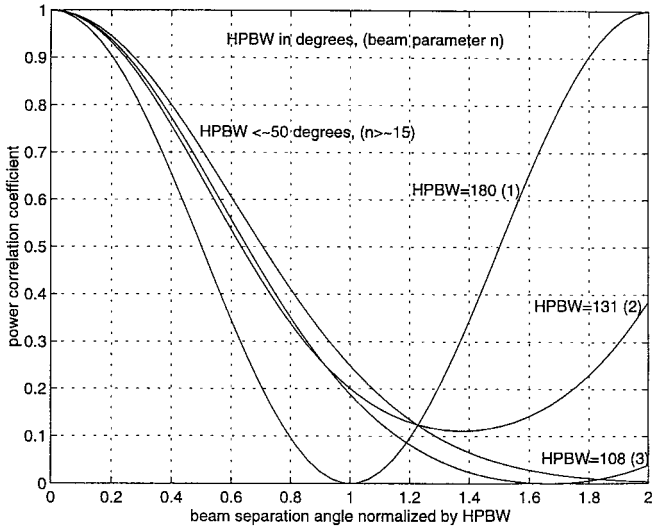

Fig. 3. The power correlation coefficient for $\cos^n$ beams including the low-gain cases of $\mathrm{HPBW} = 180°$, $131°$, and $108°$.

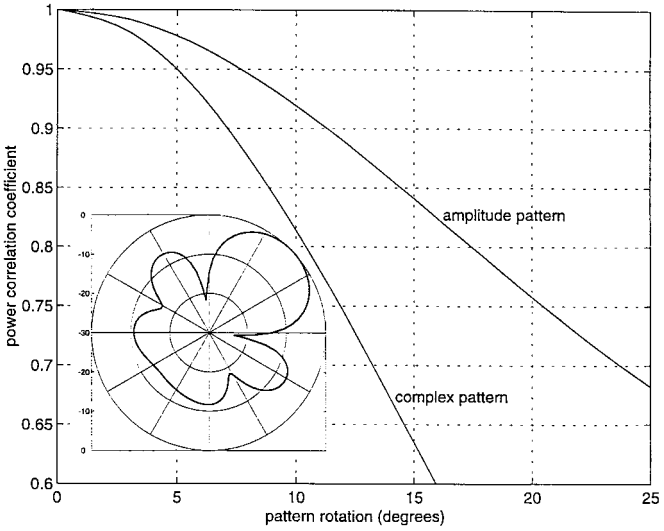

Fig. 4. The pattern and correlation coefficient function for a six-element Yagi antenna pattern. The HPBW is 52°. The upper curve is for the amplitude pattern, which gives a 0.7 decorrelation angle of 23°, and the lower curve is for the complex pattern which results in a decorrelation angle of 13°.

in which the simplification

$$I_{cc}(2n_\phi, 0) = I_c(n = 2n_\phi) = \int_{-\pi}^{\pi} \cos^n\left(\frac{\phi}{2}\right) d\phi = 2I_s(n), \quad n \text{ even} \tag{44}$$

can be used. The correlation coefficient function is then

$$\rho(\Psi) = \frac{(2n_\phi)!!}{(2n_\phi - 1)!!} \cdot \frac{1}{2^{2n_\phi - 1}} \cdot F_n\left(n_\phi, \frac{\Psi}{2}\right). \tag{45}$$

The θ dependence drops out in the normalization, as expected from the discussion of the previous section. The power correlation coefficient function $|\rho_g(\Psi)|^2 \approx \rho_e(\Psi)$ is plotted in Fig. 3 for HPBW's of 180° ($n_\phi = 1$), 131° ($n_\phi = 2$), 108° ($n_\phi = 3$), and $\mathrm{HPBW} <\sim 50°$ ($n_\phi >\sim 15$).

For this latter case of moderate and high directivities, the same rule-of-thumb that was derived for the Gaussian beams is confirmed: the $\rho_e = 0.7$ decorrelation angle is half of the HPBW of the beam. The formulation here using cosine beams addresses lower directivity patterns, which was not so convenient with the Gaussian beams. For example the beam with a HPBW of 180° has a 0.7 decorrelation angle of 0.38 times the HPBW, i.e., about 67°; for the 108° beamwidth, we get about 50° for the 0.7 decorrelation angle. The broader the low directivity cosine beam, the less the decorrelation angle relative to the HPBW becomes.

The use of directional scenarios is straightforward to incorporate in the formulation here by using cosine angular distributions, which has the effect of increasing the values of the integer powers of the sine and cosine terms in the integral for the correlation function. Increasingly directive scenarios serve to increase the decorrelation angle in the same way as with the Gaussian beams.

D. Comparison with Realistic Patterns in a Uniform Scenario

For comparison, results from the angular correlations of numerical far-field patterns from moment-method calculations

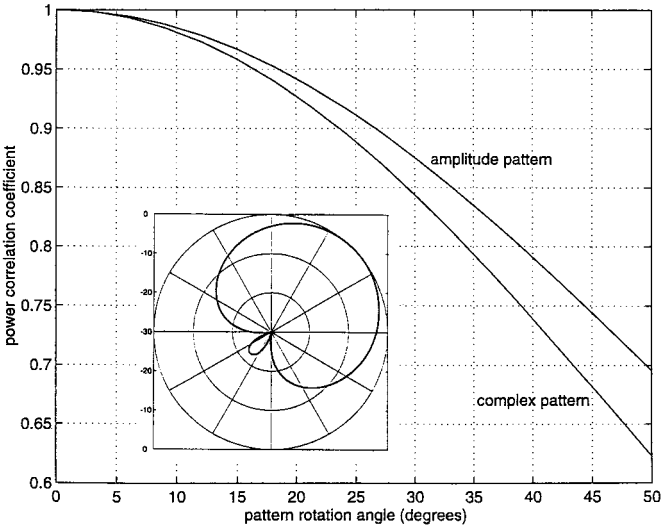

Fig. 5. A low-directivity pattern with its correlation function. The 0.7 decorrelation angle is similar for the amplitude pattern (about 50°) and for the complex pattern (about 40°).

in a uniform scenario are quoted from [11]. For a six-element Uda–Yagi antenna with a HPBW of 52°, the amplitude-only pattern gives a 0.7 decorrelation angle of 23°, which fits with the rule-of-thumb given here. The complex pattern gives a 0.7 decorrelation angle of about 13°, i.e., half that of the amplitude-only pattern. The two correlation functions are given in Fig. 4.

For a low-directivity beam, the difference between the real and complex beam results is not usually as pronounced as for a high-directivity beam with sidelobe structure, although this, of course, depends on the phase behavior of the pattern. A "well-behaved" pattern from a multiple-wire antenna and its correlation coefficient function are given in Fig. 5. The HPBW is about 90° and the 0.7 decorrelation angles are about 50° (amplitude pattern) and 40° (complex pattern).

In summary, the effect of any sidelobe structure and phase nonuniformity in the pattern is seen to decrease the decorrelation angle relative to that of the amplitude-only pattern, which is also an intuitive result. For the medium directivity pattern of the Yagi antenna, the decorrelation angle reduces to one quarter of the HPBW in a uniform scenario. This is a large change from the rule-of-thumb of half of the HPBW, which applies to amplitude-only patterns. For Gaussian beams, this means that the beam overlap moves from the 3-dB points to the 0.8 dB points. However, such directive antennas may often be operated in directive scenarios, which, from the results above and from the fact that the sidelobe structure is not normally utilized, would serve to increase the decorrelation angle to be greater than a quarter of the HPBW.

IV. Rotation of an Elliptic Beam

The study of beams in uncorrelated scenarios is concluded by the decorrelation action on elliptic beams by rotation of the beam about its boresight direction. The scenario is circularly symmetric Gaussian, centered at zenith, i.e., at $\theta = 0$

$$S(\theta, \phi) = S(\theta) = Ke^{-\frac{\theta^2}{2\sigma_s^2}} \tag{46}$$

where the normalizing constant

$$K^{-1} = 2\pi \int_0^{\pi} e^{-\frac{\theta^2}{2\sigma_s^2}} \sin\theta \, d\theta \tag{47}$$

does not require evaluation for finding the correlation coefficient. For a uniform scenario $\sigma_s = \infty$ and $S_U = \frac{1}{4\pi}$. For a single incoming wave from the zenith direction, $S_Z(\theta) = \frac{\delta(\theta)}{2\pi \sin\theta}$.

A general elliptic beam, which is suitable for rotation, can be written

$$g(\theta, \phi) = \cos^n\left(\frac{\theta}{2}\right) e^{-\frac{\theta^2}{2\sigma_g^2(\phi)}} \tag{48}$$

where the beamwidth proportional to σ_g is modulated as an elliptic function in ϕ. Specifically

$$\sigma_g^2(\phi, a^2, \chi^2) = \frac{a^2\chi^2}{\cos^2\phi + \chi^2 \sin^2\phi} \tag{49}$$

where $\chi = b/a$ and a and b are the conventional elliptic parameters. At $\phi = 0$ and π, $\sigma_g = a\chi = b$; at $\phi = \pi/2$ and $3\pi/2$, $\sigma_g = a$. Fig. 6 depicts the elliptic beams "seen" from the $\theta = 0$ direction. The correlation argument is the beam rotation angle 2γ and the ratio of the HPBW's is $\chi = R$. The scenario is circular, with beams co-centered at $\theta = 0$.

The $\cos^n \theta/2$ term is used to ensure that the beam has constant value (zero in this case) at $\theta = \pi$, i.e., in the back direction. Without the cosine term, the beam has multiple values at $\theta = \pi$ depending on ϕ, which is not physical. The HPBW's are affected by the choice of n unless $n <\sim 0.01$ in which case the cut off (where beam function approaches zero) as θ approaches π can be too sharp to model a physically realizable beam. In the following, $n = 1$, which restricts the HPBW to less than 180°. A smaller n is required for broader beams. The HPBW has to be found numerically. The equations allow straightforward use of the Newton–Raphson technique.

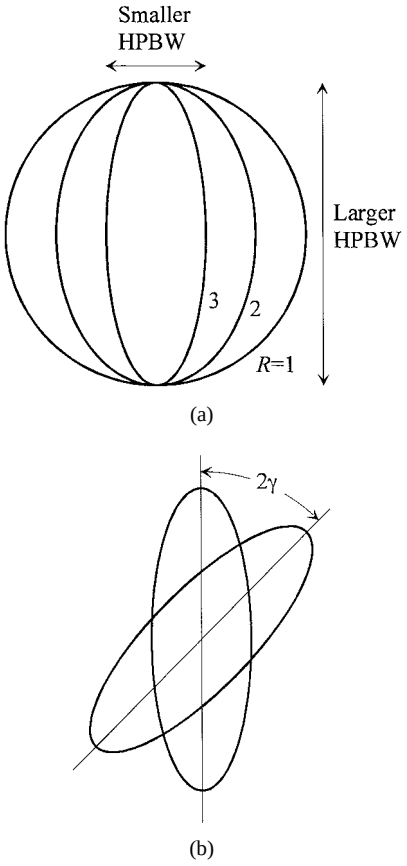

Fig. 6. (a) Indicates the elliptic beams where the ratio of HPBW's is a parameter. (b) Indicates the beam rotation about boresight as a mechanism to obtain uncorrelated signals.

For HPBW's less than about 35°, the HPBW expression for the Gaussian beams is accurate.

The correlation function for rotating the beam by 2γ in the ϕ direction is

$$R_g(2\gamma) = K \int_{-\pi}^{\pi} \int_0^{\pi} e^{-k_1(\phi,\gamma)\theta^2} \cos^2\left(\frac{\theta}{2}\right) \sin\theta \, d\theta \, d\phi \tag{50}$$

where

$$k_1(\phi, \gamma) = \frac{1}{2\sigma_s^2} + \frac{\cos^2(\phi-\gamma)+\cos^2(\phi+\gamma)+\chi^2(\sin^2(\phi-\gamma)+\sin^2(\phi+\gamma))}{2a^2\chi^2}. \tag{51}$$

No closed form was found for the integrals in the correlation functions although some simplifications can be made for special cases in order to decrease computation time. The correlation coefficient function is

$$\rho(2\gamma) = \frac{\iint e^{-k_1(\phi,\gamma)\theta^2} \cos^2\theta \sin\theta \, d\theta \, d\phi}{\iint e^{-k_1(\phi,\gamma=0)\theta^2} \cos^2\theta \sin\theta \, d\theta \, d\phi}. \tag{52}$$

This is presented as the power correlation coefficient $|\rho(2\gamma)|^2 \approx \rho_e(2\gamma)$ as a function of the rotation angle 2γ and with the ratio of the HPBW's of the elliptic beams as a parameter.

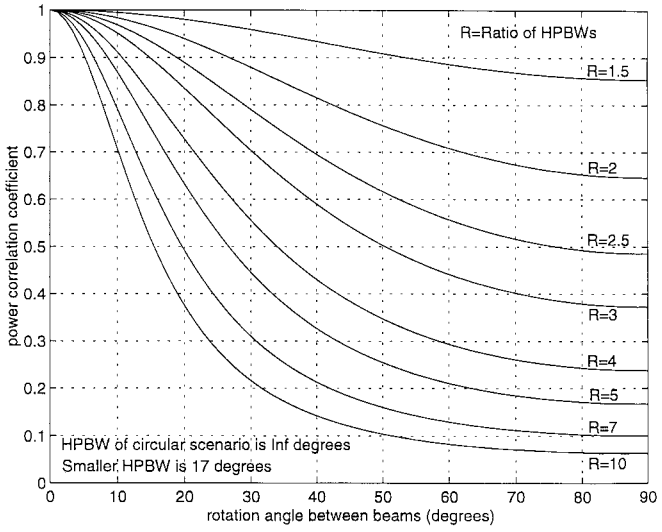

(a)

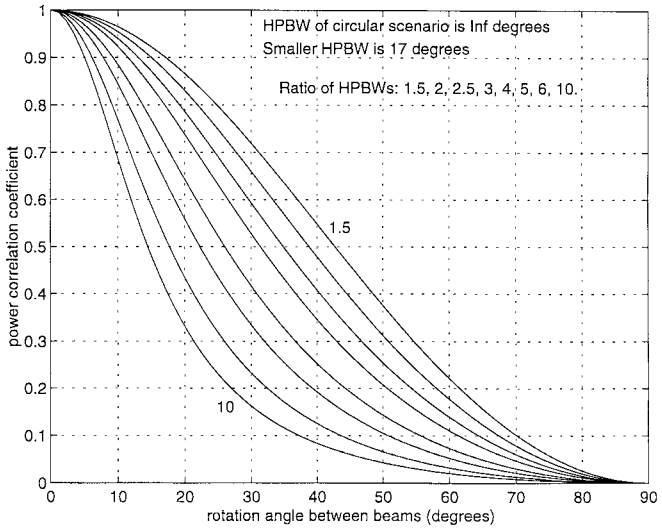

(b)

Fig. 7. An example of the envelope correlation functions. The rotation angle is the angle between the two co-directed identical elliptic beams that have a ratio of HPBW's of R. The scenario is uniform and here the smaller HPBW is fixed at 17°. (a) Scalar beams. (b) Vector case, which corresponds to the scalar beam curves being multiplied by $\cos^2$ (rotation angle).

The rotation of the beam corresponds to including the effect of linear polarization diversity when the beam is purely polarized and recall here that the polarizations in the scenario are assumed uncorrelated. The relationship between the correlation coefficient for the scalar and vector cases is

$$|\rho^{(v)}|^2 = |\rho^{(s)}|^2 \cos^2(2\gamma). \tag{53}$$

The vector case always has a zero correlation coefficient for a rotation of 90°, which corresponds to receiving orthogonal linear polarizations that are (postulated as) uncorrelated. Fig. 7(a) and (b) shows an example of the decorrelation function for a scalar and vector beam, respectively. The scalar case also applies to circularly polarized beams where a beam rotation is inconsequential in the sense that it just changes the (circularly polarized) received signal contributions by a phase factor given by the rotation angle.

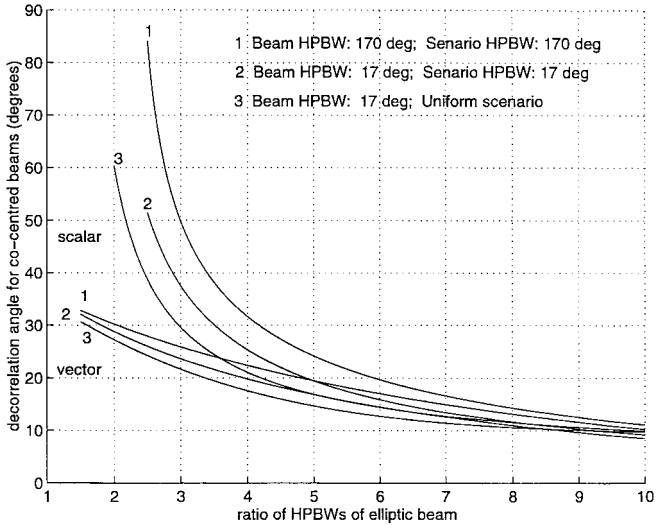

Fig. 8. The 0.7 decorrelation angle for scalar (upper set) and vector (lower set) real elliptic beams.

The curves are similar for low directivity (HPBW 170°) and also for scenario spreads reducing to the same HPBW as the larger HPBW of the beams.

The $\rho_e = 0.7$ decorrelation values are presented as a function of the ratio of the HPBW's in Fig. 8. Curve 1 is for low directivity (HPBW 170°) and can be compared with beam 2, the high directivity (HPBW 17°) case. For both 1 and 2, the scenario HPBW is the same as the larger HPBW of the beams. The main difference occurs at low HPBW ratios where the decorrelation angles are a maximum of about 35° apart.

The vector cases are all rather similar indicating that the uncorrelated linear polarizations is the dominant decorrelating effect for lower HPBW ratios of the beam, as expected. Even for beams with a HPBW ratio as low as 1.5, a beam rotation of about 30° is sufficient for decorrelating the signals. For HPBW ratios of greater than about five, the curves for the scalar and vector cases are almost the same. Here, the (scalar) pattern rotation is the principle decorrelation mechanism, not the uncorrelated polarizations of the scenario.

V. Conclusion

The conditions for angle diversity have been established for antenna beams that are purely real. The uncorrelated distributed scenario is weighted to incorporate the effects of directive angle-of-arrival found in actual situations. Numerical complex patterns are also evaluated in a uniform uncorrelated scenario to show the effect of sidelobe structure and phase nonuniformity.

The decorrelation angle for real beams in a uniform scenarios is shown to be half of the half-power beamwidth. This is rule-of-thumb can be used for configuring multiple-beam base-station diversity antennas and is independent of the directivity as long as the HPBW is less than about 90° (directivity less than ∼6 dB). The presence of sidelobes and

the fact that a real-world pattern is complex rather than real can result in a reduction of the decorrelation angle by a factor of up to a half, i.e., to one quarter of the half-power beamwidth, in a uniform scenario. Directive scenarios result in an increase of the decorrelation angle. The formulation for the rotation of elliptic beams in a circular Gaussian scenario give guidelines for the decorrelation angles for both scalar and elliptic beams.

REFERENCES

[1] D. E. Kerr, Ed., *Propagation of Short Radio Waves*. New York: McGraw-Hill, vol. 13, 1951 (Radiation Lab. Series).

[2] W. C. Jakes, Ed., *Microwave Mobile Communications*. New York: Wiley, 1974; IEEE Press, 1993.

[3] R. G. Vaughan and J. B. Andersen, "Antenna diversity in mobile communications," *IEEE Trans. Veh. Technol.*, vol. VT-36, pp. 149–172, Nov. 1987.

[4] R. H. Clarke, "A statistical theory of mobile radio reception," *Bell Syst. Tech. J.*, vol. 47, pp. 957–1000, 1969.

[5] J. R. Pierce and S. Stein, "Multiple diversity with nonindependent fading," *Proc. IRE*, vol. 48, pp. 89–104, Jan. 1960.

[6] W. C.-Y. Lee and Y. S. Yeh, "Polarization diversity system for mobile radio," *IEEE Trans. Commun.*, vol. C-20, pp. 912–923, Oct. 1972.

[7] R. G. Vaughan, "Polarization diversity in mobile communications," *IEEE Trans. Veh. Technol.*, vol. 39, pp. 177–186, Aug. 1990.

[8] R. G. Vaughan, J. B. Andersen, and M. H. Langhorn, "Circular array of outward sloping monopoles for vehicular diversity antennas," *IEEE Trans. Antennas Propagat.*, vol. 36, pp. 1365–1374, Oct. 1988.

[9] R. G. Vaughan and N. L. Scott, "Closely spaced monopoles for mobile communications," *Radio Sci.*, vol. 28, no. 6, pp. 1259–1266, Nov./Dec. 1993.

[10] J. D. Kraus, *Antennas*, 1st ed. New York: McGraw-Hill, 1950, 2nd ed., 1988.

[11] R. G. Vaughan, "Switched parasitic elements for antenna diversity," submitted to *IEEE Trans. Antennas Propagat.*

Rodney G. Vaughan (M'84–SM'89) received the B.E. and M.E. degrees from the University of Canterbury, New Zealand, in 1975 and 1976, respectively, and the Ph.D. degree from Aalborg University, Denmark, in 1985, all in electrical engineering.

In 1972, he joined the New Zealand Post Office (now Telecom NZ Ltd.) where he worked on communications network analysis and telephone traffic forecasting. In 1978 he joined the Physics and Engineering Laboratory of the New Zealand Department of Scientific and Industrial Research (DSIR), Lower Hutt, where he helped to pioneer New Zealand industrial applications of microprocessor technology including the development of tools for real-time software and the design and development of electronic scientific and industrial equipment ranging from hardware solutions to software protocol simulators for networks. In 1990 he was transferred to the Physical Sciences Division of DSIR, in 1991 to the Industrial Development Division of the DSIR, and in 1992 to the New Zealand Institute of Industrial Research Limited (NZIIRL, formerly part of the DSIR). While with the DSIR, he initiated and developed a formal research program on communications technology, which received funding from the New Zealand Foundation for Research, Science, and Technology (FRST). He founded the Communications Team at IRL and was Team Leader until 1995, managing several scientific and industrial research projects. He was an URSI Young Scientist and from 1995 to 1996 he worked at the Center for PersonKommunikation at Aalborg University, Denmark. Currently, he is Program Leader of Communications Signal Processing and Cosupervisor of Ph.D. thesis projects. His research interests in the IRL Communications Team encompass personal and satellite communications with projects on multipath communications theory (electromagnetic, line, and acoustic media), diversity design, signal and sampling theory, and signal processing. Recent industrial projects have included the design and development of specialist antennas for personal and satellite communications. He is also involved in research of multipath propagation mechanisms, multipath analysis and prediction, space–time processing, DSP application, and optimum multiport antennas. He has several patents in the antennas and signal processing field.

Dr. Vaughan is a registered engineer in New Zealand, an URSI Correspondent, and the New Zealand Secretary for URSI. In 1982 he received a DSIR Public Service Study Award.